AFRL-RX-TY-TP-2010-0050

A NEURAL-NETWORK MODEL-BASED ENGINEERING TOOL FOR BLAST WALL PROTECTION OF STRUCTURES (POSTPRINT)

Bryan T. Bewick
Airbase Technologies Division
Air Force Research Laboraotry
139 Barnes Drive, Suit 2
Tyndall Air Force Base, FL 32403-5323

Ian Flood
University of Florida, 338 RNK
Gainesville, FL 32611

Zhen Chen
University of Missouri-Columbia
E2509 Lafferre Hall
Columbia, MO 65211

Contract No. FA4819-09-C-0032

June 2011

AIR FORCE RESEARCH LABORATORY
MATERIALS AND MANUFACTURING DIRECTORATE

■ **Air Force Materiel Command** ■ **United States Air Force** ■ **Tyndall Air Force Base, FL 32403-5323**

REPORT DOCUMENTATION PAGE

Form Approved
OMB No. 0704-0188

PLEASE DO NOT RETURN YOUR FORM TO THE ABOVE ADDRESS.

1. REPORT DATE *(DD-MM-YYYY)*	2. REPORT TYPE	3. DATES COVERED *(From - To)*
30-JUN-2011	Journal Article - POSTPRINT	01-MAY-2009 -- 10-MAY-2010

4. TITLE AND SUBTITLE

A Neural-Network Model-Based Engineering Tool for Blast Wall Protection of Structures (POSTPRINT)

5a. CONTRACT NUMBER

FA4819-09-C-0032

5b. GRANT NUMBER

5c. PROGRAM ELEMENT NUMBER

0602102F

6. AUTHOR(S)

*Bewick, Bryan; ^Flood, Ian; ^^Chen, Zhen

5d. PROJECT NUMBER

4915

5e. TASK NUMBER

F2

5f. WORK UNIT NUMBER

Q210FA72

7. PERFORMING ORGANIZATION NAME(S) AND ADDRESS(ES)

^Rinker School of Building Construction, University of Florida, 338 RNK, Gainesville, FL 32611;
^^Department of Civil and Environmental Engineering, University of Missouri, E2509 Lafferre Hall, Columbia, MO 65211

8. PERFORMING ORGANIZATION REPORT NUMBER

9. SPONSORING/MONITORING AGENCY NAME(S) AND ADDRESS(ES)

* Air Force Research Laboratory
Materials and Manufacturing Directorate
Airbase Technologies Division
139 Barnes Drive, Suite 2
Tyndall Air Force Base, FL 32403-5323

10. SPONSOR/MONITOR'S ACRONYM(S)

AFRL/RXQEM, AFRL/RXQF

11. SPONSOR/MONITOR'S REPORT NUMBER(S)

AFRL-RX-TY-TP-2010-0050

12. DISTRIBUTION/AVAILABILITY STATEMENT

Distribution Statement A. Approved for public release; distribution unlimited.

13. SUPPLEMENTARY NOTES

Ref AFRL/RXQ Public Affairs Case # 10-092, 26 May 2010. Document contains color images. Published in International Journal of Protective Structures, Vol 2, No 2 (2011), pp 159-176.

14. ABSTRACT

Blast barrier walls have been shown to reduce blast loads on structures, especially in urban environments. Analysis of existing test and simulation data for blast barrier response has revealed that a need still exists to determine the bounds of the problem and produce a fastrunning accurate model for the effects of barrier walls on blast wave propagation. Since blast experiments are very time intensive and extremely cost prohibitive, it is vital that computational capabilities be developed to generate the required data set that can be utilized to produce simplified design tools. The combination of high fidelity model-based simulation with artificial neural network techniques is proposed in this paper to manage the challenging problem. The proposed approach is demonstrated to estimate the peak pressure, impulse, time of arrival, and time of duration of blast loads on buildings protected by simple barriers, using data generated from validated hydrocode simulations. Once verified and validated, the proposed neural-network model-based simulation procedure would provide a very efficient solution to predicting blast loads on the structures that are protected by blast barrier walls.

15. SUBJECT TERMS

explosion, blast barriers, blast walls, blast loads, neural networks, model-based simulation

16. SECURITY CLASSIFICATION OF:			17. LIMITATION OF ABSTRACT	18. NUMBER OF PAGES	19a. NAME OF RESPONSIBLE PERSON
a. REPORT	b. ABSTRACT	c. THIS PAGE			Paul Sheppard
U	U	U	UU	19	19b. TELEPHONE NUMBER *(Include area code)*

Reset

Standard Form 298 (Rev. 8/98)
Prescribed by ANSI Std. Z39.18

A Neural-Network Model-Based Engineering Tool for Blast Wall Protection of Structures

by

Bryan Bewick, Ian Flood and Zhen Chen

Reprinted from

International Journal of

Protective Structures

Volume 2 · Number 2 · June 2011

Multi-Science Publishing

ISSN 2041-4196

A Neural-Network Model-Based Engineering Tool for Blast Wall Protection of Structures

Bryan Bewick[1,*], Ian Flood[2] and Zhen Chen[3]
[1]Air Force Research Laboratory, 139 Barnes Drive, Suite 2, Tyndall AFB, FL, 32403, USA
[2]Rinker School of Building Construction, University of Florida, 338 RNK, Gainesville, FL 32611, USA
[3]Department of Civil and Environmental Engineering, University of Missouri, E2509 Lafferre Hall, Columbia, MO 65211, USA

Received on 16 June 2010, Accepted on 28 Jan 2011

ABSTRACT
Blast barrier walls have been shown to reduce blast loads on structures, especially in urban environments. Analysis of existing test and simulation data for blast barrier response has revealed that a need still exists to determine the bounds of the problem and produce a fast-running accurate model for the effects of barrier walls on blast wave propagation. Since blast experiments are very time intensive and extremely cost prohibitive, it is vital that computational capabilities be developed to generate the required data set that can be utilized to produce simplified design tools. The combination of high fidelity model-based simulation with artificial neural network techniques is proposed in this paper to manage the challenging problem. The proposed approach is demonstrated to estimate the peak pressure, impulse, time of arrival, and time of duration of blast loads on buildings protected by simple barriers, using data generated from validated hydrocode simulations. Once verified and validated, the proposed neural-network model-based simulation procedure would provide a very efficient solution to predicting blast loads on the structures that are protected by blast barrier walls.

1. INTRODUCTION

Blast barrier walls are often implemented as an integrated protective element for increasing the level of protection for a structure or facility. When designed carefully, they can increase the level of protection for a structure or facility in several ways. The main protection is provided by the standoff between the threat and the structure or facility, since blast waves have been shown to decay exponentially with distance [1]. A second advantage is that blast walls can greatly reduce the blast loads in the environment immediately behind them [2].

*Corresponding author. E-mail address: bryan.bewick@tyndall.af.mil

This occurs because the blast pressure wave is forced to propagate over the height of the blast wall (reflecting some of the energy away from the building) and then expand back down the other side towards the ground (thereby dispersing more of the energy). Yielding of the barrier will also absorb some of the energy. In this case, the biggest advantage is attained by making the blast wall similar in height and close in proximity to the structure being protected. If the blast wall is too far away from the structure, the advantage of having a large standoff is attained (that of decay in the concentration of its energy), but the blast wave has time to build back to a uniform shock front propagating along the ground and the loads to the structure will be similar to the configuration where no blast barrier wall is present.

Predicting blast loads on structures in an open air environment is something that is well understood [10] and is captured by existing prediction methodologies which will be referred to as the TM5-1300 method [1]. However, the solution to blast loads on structures is greatly complicated by the presence of a blast barrier wall. Blast pressures and impulse are reduced due to the reflection and dispersion of some of the wave's energy by the barrier. On the other hand, peaks and troughs in the blast loading across the face of the building can result from interference between the leading wave and the portion of it reflected off the ground behind the barrier. This configuration is a non-linear problem. Depending on the specific configuration of the charge weight, W, the charge to barrier standoff, d_1, the charge to structure standoff, Z, and the barrier height, H, (Figure 1), there are multiple reflections of the blast wave that occur in the problem. For small barrier to building standoff configurations, there are at least two spikes in the reflected pressure loading the structure; one for the direct line of the shock front propagating over the barrier wall and directly towards any point on the structure, and a second where the shock front propagates back to the ground and then reflects onto the structure. The effect is lessened at higher locations vertically on the structure. Additional significant spikes can occur when the shock front reflects back and forth between the building and the barrier. As the barrier to structure

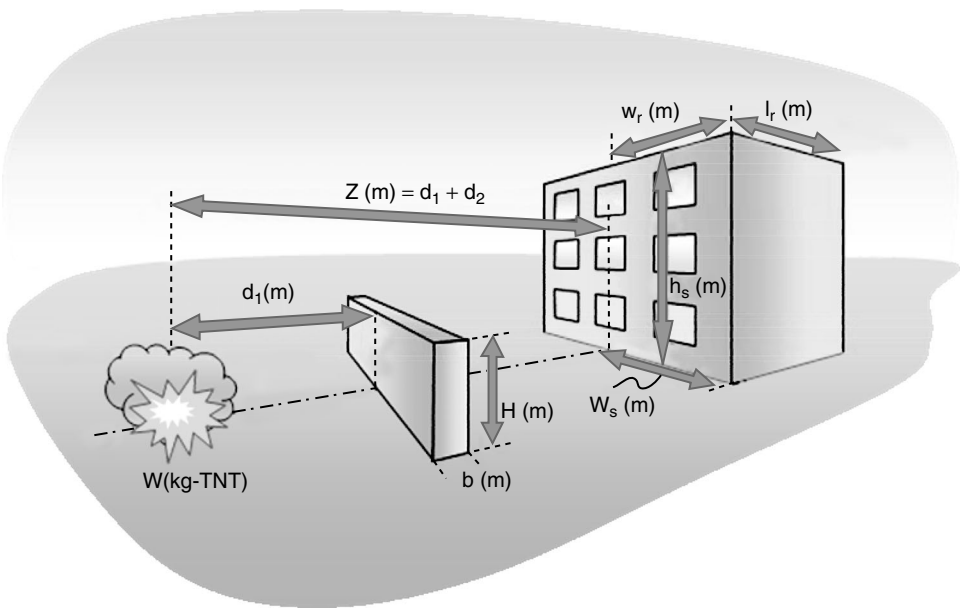

Figure 1. Blast barrier wall configuration

standoff is increased, the structure loads begin to resemble loads in the free-field blast propagation configuration. The complexity of the problem requires enhanced multivariate, non-linear tools for modeling and analysis.

One approach to predicting blast loads with protective blast walls includes case-specific computational modeling with software such as LS-DYNA [12], AUTODYN [13], FEFLO [14], Air3D [15], SHAMRC [16], CTH [18], and DYSMAS [19]. The downside to this approach is the logistics of performing such simulations while ensuring the accuracy of the predictions. If there is a single facility site configuration to evaluate, then this might be a good approach for an experienced computational modeler to perform. If there are multiple cases to be considered, i.e. differing standoffs, charge sizes, and blast wall heights, then a simulation modeling approach becomes very cumbersome and time consuming. Even using the most powerful of multi-processor based supercomputers, the simulations can take days or weeks to execute [20]. Moreover, supercomputers are typically shared resources and may incur lengthy wait times before a job is processed, further increasing the time before output of results. Studies attempting to reduce the time required to execute a simulation by using a much coarser spatial mesh for the models have shown errors as much as 50% [21].

An alternative approach that can produce estimates of peak pressure and impulse extremely quickly (in a fraction of a second) uses empirically derived curves hand-crafted to fit data gathered from a set of experiments. Specifically, experimental data have been used to develop rules and factors for adjusting the estimates from the TM5-1300 method of predicting loads on structures in free-field blast configurations. Rose et al. [2] applied this technique to data gathered from small scale experiments to generate prediction charts. This technique was outlined in UFC 4-020-03 [4] and is a very common approach used in the blast community when dealing with blast walls. Bogosian et al. [5] added 40 live blast tests to the data from the Rose et al. work to expand the bounds of the prediction method. The approach shows ranges of accuracy. The methods produce higher values of uncertainty for pressure than for impulse. Rickman et al. [7] conducted a series of experiments and computational simulations at approximately 1:18 and 1:30 scales used to develop curve-fitted models of blast barrier effectiveness. The final product from the Rickman et al. experiments was a series of adjustment factors for pressure and impulse loadings with a blast wall present. The work further expanded the bounds of the prediction method as based upon the work of Rose et al. and Bogosian et al. Zhou and Hao [9] took a similar approach, but used simulation models (based on AUTODYN), rather than live experiments, to generate a database of pressure-time histories over the height of a structure for a range of blast barrier wall configurations. A series of logical rules were generated to select from a set of curves based on observations from these simulations. The above empirical models were evaluated using the same data used to generate the model, or using a very small sample of problem configurations. As such, more work is required to validate their performance across the entire problem domain.

Artificial neural networks (ANNs) have also been used as an empirically based method for modeling the blast loads on structures behind a protective blast barrier wall. Compared to the hand-crafted curve fitting approach discussed above, ANN's have the advantage that they can develop much more intricate and thus accurate curves to fit a set of experimental observations, and they do this automatically. In fact, in principle, there is no limit to the complexity of the curves (or hyper-surfaces in the case of multivariate problems) that an ANN can develop or to the number of independent variables they can consider, given sufficient training data and computing resources (such as memory and processing time) [22]. However, the approach also has similar restrictions in that it requires a large data set to accurately develop the models, and

the models are not able to extrapolate well beyond the bounds of the experimental data. Moreover, as is usually the case with empirical methods, the number of observations required to develop a model tends to increase geometrically with the number of independent variables describing the problem thus placing a practical limit on the complexity of the problem that can be considered. Remennikov and Rose [24] developed an ANN-based model that covered several of the values represented in Figure 1 (d_1, Z, and H) as well as the height of burst (HOB) and the height of measuring point behind the barrier wall, using data from miniature scale experiments for free-field propagation behind a barrier without a reflective structure. The model output the peak scaled pressure and the peak scaled impulse. The model showed good correlation with the data, but had a limited range of applicability due to the distribution of the available training data. Similar work has been performed by the authors of this paper exploring the capability of a radial Gaussian (RGIN) neural networking method, using existing live experimental data [20]. The study found that existing data is too sparse and does not provide a good even distribution of the variable space.

Of the direct modeling methods that have been developed for estimating the blast loading on buildings, ANNs appear to have the greatest potential. As with all direct estimation models, they can generate results in a fraction of a second thereby allowing optimal blast mitigation designs to be found within a reasonable period of time. Moreover, they can in principle develop solutions to nonlinear problems to any degree of accuracy (given sufficient data and training) and they can consider any number of independent variables within a model. However, as with all empirically-based direct modeling methods, there is a practical limitation to the approach resulting from the quantity of data required to develop a model which tends to increase geometrically with the number of independent variables. This effectively limits the level of accuracy that can be achieved and the range of problems that can be considered. Existing studies have not tested the practical limits of this technology, and many of them have failed to provide a thorough and balanced validation of their performance. The objective of this study is to address this issue and thereby identify the true potential of ANN-based direct estimation of blast loading on buildings.

2. METHODOLOGY

The approach is to populate data through numerical simulations in order to generate an accurate and efficient ANN model-based engineering tool. The idea behind a neural network is that it fits a surface (or hypersurface) to a set of observations of the performance of the real system. Neural networks have many benefits. They work well with large numbers of independent variables and highly non-linear problems; and can be trained to output a variety of solutions.

The approach for the current study is to populate a $3 \times 3 \times 3 \times 3$ grid of the data variable space using computational modeling. In other words, a range of three values was used for each of the four main independent variables. The limitation of this approach is the exclusion of certain variables. Eight independent variables were considered in this study as illustrated in Figure 1; W, d_1, Z, H, w_s, w_r, h_s, *and* l_r. with the thickness of the barrier, b, set constant at 0.3 m The four main independent variables used are W, d_1, Z, and H. Two other dependent variables(either w_s, and h_s, or w_r, and l_r, which define a position on the front of the structure or its roof, respectively) will be input into the ANN, but they do not affect the number of simulations required as these data points are inherently captured within the confines of each simulation. In order to completely cover the data space, the number of data points required is determined by the number of data points in the variable space grid raised to the power of the number of independent variables. This means that a data set of 81 (3^4) experiments is required to fully encapsulate the variable space for a $3 \times 3 \times 3 \times 3$ grid.

Table 1. Range of values for the six independent variables

	Min	**Max**
W TNT (kg)	22.68	910.42
d_1 (m)	0	7.62
Z (d_1 + d_2) (m)	3.048	30.48
H (m)	1.52	6.1
h_s (m)	0	9.144
w_s (m)	0	1.52
b (m)	0.3	0.3
l_r (m)	0	1.524

The scope entails a setup of 91 experiments of which 81 simulations were used to populate data with appropriate blast barrier configurations to train the neural network models. The other 10 simulations were used to verify and validate the accuracy of the neural network. The ranges for the series of experiment configurations are shown in Table 1 – these values were selected to encompass the majority of configurations encountered in the field. The structure width, w_s, and structure height, h_s, (or roof width, w_r, and roof length, l_r) are shown as varied values to allow the neural network to produce loadings at any point on the face (or roof) of the structure. Separate ANN models were developed for predicting peak pressure, impulse, time of arrival for the peak pressure, and the positive phase duration of the applied blast loads on the face of the structure and on the roof of the structure. Other parameters (such as the width of the building – which was considered to be infinite) were not treated as variables to keep the data set required to develop model at a reasonable size.

The ANN training data included a grid of data history points on the surfaces where predictions were desired. For the structure face, a 6×31 grid of data points for a total of 186 data points were collected from each experiment. For the roof models, a 6×6 grid of data points were generated giving a total of 36 data points. The ANN can then predict the results at any point within the bounds of the defined variable space in Table 1. For the roof loading, data were collected only for the first 1.524 m of the roof. The barrier wall was considered to be infinitely long, so there would be no wrap-around effects included.

3. NUMERICAL SIMULATION

There are several existing computational codes which have invested much effort into the capability to accurately model the blast environment. The codes considered are first-principle model-based approaches that model the detonation and burn of explosive materials, and the energy transferred into a blast wave. SHAMRC [16], CTH [18], and DYSMAS [19] have been evaluated for the current effort. CTH and SHAMRC are hydrocodes that have been used extensively for blast modeling [25]. DYSMAS is a hydrocode that was developed for underwater explosions. It features a fluid solver, GEMINI [27], coupled with a US Navy version of DYNA2D. While DYSMAS has been used extensively and validated for underwater explosion events, there is little work with the code for explosions in air, although it has been used with success for modeling a blast event of a field fortification [28].

Verification and validation of numerical software provide engineers with the tools to bound the amount of error that might be expected in a given simulation. A mesh convergence study has been performed in this project to compare the accuracy and performance of each selected code. The error and mesh size requirements have been compared using the idea of a grid convergence

index (GCI) [29]. A 2D-axisymmetric comparison of CTH, SHAMRC and DYSMAS has been performed by considering a free-field airblast problem. The results are also compared against existing work determining a GCI for LS-DYNA, CTH, and AUTODYN [31].

Results from the two studies showed that LS-DYNA, CTH, and DYSMAS appear to be good options in regard to the rate of convergence and accuracy for both pressure and impulse. Due to the volume of data required to train the desired neural networks, an efficient scalable code is desired. DYSMAS has ultimately been chosen due to its superior performance in regards to the trade-offs between the efficiency and accuracy for creating a large database of simulation results.

For validation of the accuracy, the simulation of a live blast experiment was considered. The problem chosen was performed by the Air Force Research Laboratory at Tyndall AFB, FL. The experiment setup includes a metal revetment blast barrier wall in front of a rigid faced structure. The computational domain for modeling the blast barrier configuration was set up with a half symmetry model. The bare explosive charge was placed as a hemispherical charge on the ground level. The planes that do not act as planes of symmetry were modeled using outflow boundary conditions. Figure 2 shows the overlay of the simulation results as

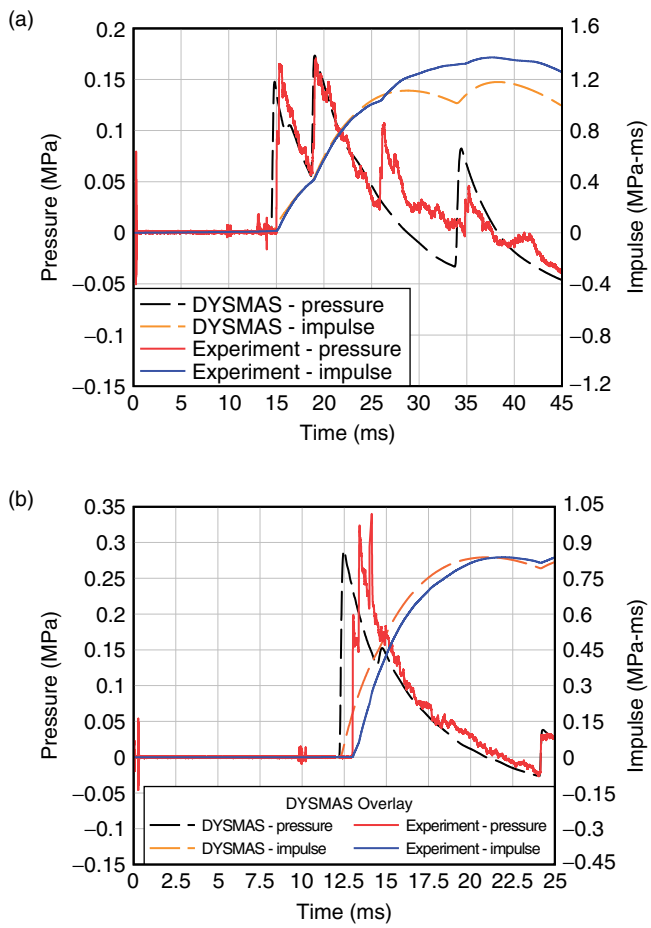

Figure 2. Overlay of reflective pressure gauges at the (a) base of the structure and (b) at mid-height

compared with the live blast data gathered from reflective pressure gauges. As can be seen, the peak pressures are predicted very well, while the impulse shows a little more variation.

4. NEURAL NETWORK DEVELOPMENT

4.1. BLAST BARRIER SIMULATION PROBLEM SETUP

The convergence studies and live blast data validation experiments provided confidence in the accuracy of DYSMAS for modeling blast shock wave propagation. For this reason, the study was carried out using DYSMAS. For each simulation completed in the current study, a common format was used. The blast wall simulations were all set up as half symmetry. For each simulation, the standoff behind the bare hemispherical surface charge opposite the blast wall was set to 1.524 m. The width of the simulation was also set to 1.524 m (correlates to w_s) due to restrictions of performing large numbers of memory intensive simulations. The structure height, h_s, was set to 9.144 m due to the restrictions of the number of input variables the ANN could manage without requiring an excessive number of training patterns. The thickness of the blast barrier, b, was set to 30.48 cm as a sensitivity study found that the thickness of the blast wall has only a minor effect on the blast load to the structure behind the blast wall. Refer to Figure 1 for domain configuration and variable definitions.

Tracer data collection points were collected at evenly spaced increments on the face of the barrier, the face of the structure, and on the first 1.524 m of the roof of the structure. The data tracer points were placed at 30.48 cm increments on each face. On the structure face, there were 31 tracer points over the height of the structure and 6 tracer points over the width for a total of 186 data collection points on the structure face for each simulation. On the roof structure, an evenly spaced grid had 6 tracer points over the length, and 6 tracer points over the width for a total of 36 tracer points

In order to produce a model with a good all-round performance, it is important to train the ANN with data that covers all regions of the variable space. As outlined in Table 1, there are nine independent variables to this problem, six of which are considered as inputs to the ANN model: W, d_1, Z, H, and either (h_s and w_s) or (l_r and w_r) – the latter choice depends whether the model represents the front face of the building or its roof. Two of these, the locations on the structure face h_s and w_s (or l_r and w_r) are inherent in each simulation and, thus, do not require extra simulations to fill that part of the variable space. Generally, experience shows that collecting data that covers a grid configured such that there are 3 values on each variable axis of the data space is required at a minimum to get accurate results from an ANN model. Moving to denser grids will provide extra information that will usually allow the ANN to develop a more accurate model although this can be quite cumbersome. In order to completely cover the data space, the number of data points required is determined by the number of data points in the variable space grid raised to the power of the number of independent variables. For the current study, there are four independent variables. Thus, for a $3 \times 3 \times 3 \times 3$ grid, there are $3^4 = 81$ simulations required. To collect enough data for a $5 \times 5 \times 5 \times 5$ grid would require $5^4 = 625$ simulations. Due to the sheer volume of computational memory and time required, this study focused on developing the $3 \times 3 \times 3 \times 3$ grid with 81 simulations. An additional 10 simulations were completed at randomly selected points in the variable space; 5 as test conditions, and 5 used to show the effect of increasing the density of data points.

This study has considered four main approaches to the problem. In each case, training of the ANN models was performed using a sample of the data collected from each simulation. For the structure face, data from 36 of the 186 tracer points were used to develop the training patterns. In the first approach presented, an evenly spaced 6×6 grid of the tracer points on the structure face was used to train the ANN model. The effects of using blast scaling were

also explored. The second approach considered the effect of biasing the collection of data from the grid on the structure faces to collect more data in the ranges that showed the greatest error from approach one. In approach three, an assessment was made of the effect of using additional simulations to increase the density of the training patterns in the variable space. An additional 5 randomly generated simulations were used to generate these additional training patterns. The fourth focus area examined the effect of blast walls on the roof loads. For the roof portion, 9 of the 36 tracer points collected in each simulation on the surface of the roof were used for training purposes.

4.2. APPROACH ONE: EVENLY SPACED TRAINING GRID

The first approach was to train four ANNs for predicting peak pressure, p (MPa), impulse, i (MPa-ms), time of arrival, toa (ms), and positive phase duration, t_{dur} (ms), respectively using training data based on an evenly spaced grid on the structure face. The independent input variables were d_1 (m), Z (m), h (m), and W (kg-TNT) and the height, h_s (m) and width, w_s (m) on the structure face The ANNs were trained using data from the primary 81 simulations performed.

The specific type of ANN adopted for this study was RGIN, a radial Gaussian architecture with an incremental learning paradigm [22]. RGIN networks function as a three layer feed forward system. The three layers are the input variables, hidden neurons, and the output variable. RGIN networks represent the data as a composite of radial-Gaussian functions. The hidden neuron portion of the feed forward system represents the number of radial-Gaussian functions used to fit the data. Each time a hidden neuron is added, a new radial-Gaussian function is added onto the system to capture the section of the problem with the largest residual errors. Development of an RGIN network progresses one hidden neuron at a time. Each hidden neuron is added so that the centroid of its radial Gaussian function is positioned over the largest error data point, its amplitude is equal to that error, and its spread is set to a value that reduces the sum of the absolute values of all residual errors as much as possible. The RGIN approach has been shown to work well with large sets of data [20]. A schematic of this type of network for a single independent variable is illustrated in Figure 3 where the dashed blue curves each represent the function implemented by a single hidden neuron, the red line is the combined output from the network, and the asterisks represent the target points for training.

Initial testing of ANN models was conducted with data from tracer points in between those used for training. Since this is not a fully accurate depiction of the validity for the ANN models, this approach was used for qualitative comparison of the different approaches to the ANN models. Figure 4 shows the training progress of the ANN approach to predicting the

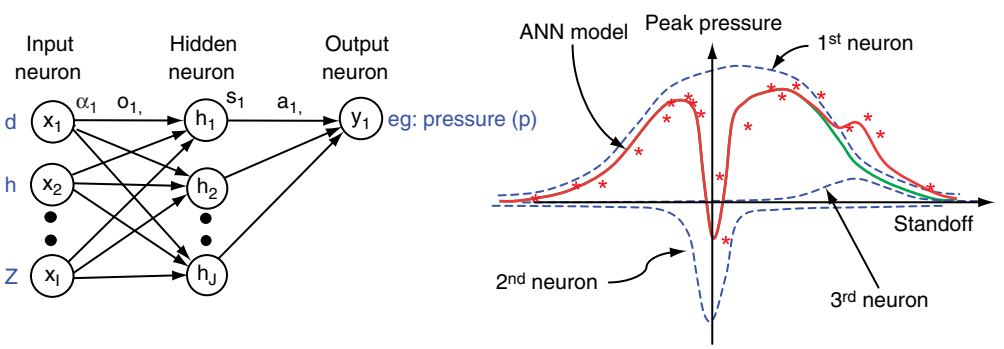

Figure 3. Schematic of RGIN neural network

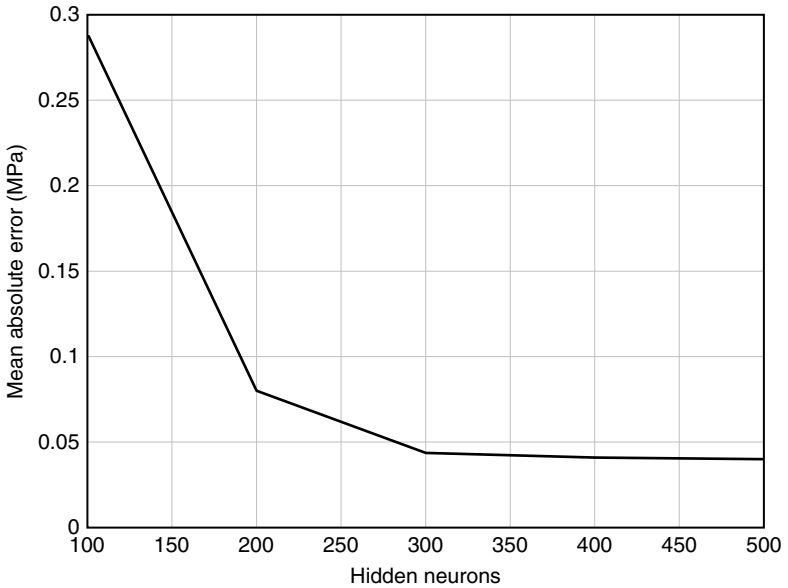

Figure 4. Training progress for RGIN ANN on impulse load to structure prediction

impulse loading to the structure face. It is typical of the results for the other three ANN models for the impulse, time of arrival, and positive phase duration. The mean absolute error was 40 kPa-ms, which relates to about 6% error. The correlation factor for each ANN was 0.9814, 0.9938, 0.9681, and 0.9806 for the peak pressure prediction, impulse prediction, positive phase duration prediction, and time of arrival prediction respectively. The mean absolute error for each ANN was 0.644 MPa, 0.040 MPa-ms, 2.22 ms, and 0.864 ms for the peak pressure prediction, impulse prediction, positive phase duration prediction, and time of arrival prediction respectively.

The initial ANN development showed very good correlation with the sample data points. One point of interest to be considered is the effect of using blast scaling. Blast scaling is a common practice for reducing the number of input variables and simplifying blast problems [1]. It is also commonly used to alter full-scale experiments into small-scale experiments. This practice helps cut costs for construction, and the difficulty of having large scale ranges capable of performing large scale detonations. The blast scaling concept relates all dimensions of a blast configuration through the charge weight by scaling the distances by $W^{-1/3}$. Cubed root scaling removes the charge weight as a variable. This concept has been used with reasonably good correlation for several other blast wall effectiveness efforts [2]. The expectation was that with fewer input variables, the ANN might be able to converge on an acceptable solution more quickly for a given number of hidden neurons (radial-Gaussian functions). Figure 5 shows the results of the ANN models trained with 500 hidden neurons for both the scaling and non-scaling versions of the network. While both results show good correlation, the scaled version has more errors in the mid and low peak pressure range. This does not show in the correlation coefficient since most of the errors are in the low and mid range biasing the measure of the correlation coefficient. Also, the non-scaled version has a higher kurtosis, meaning that the errors are a factor of a few outlier data points as opposed to many moderate sized errors as in the scaled version.

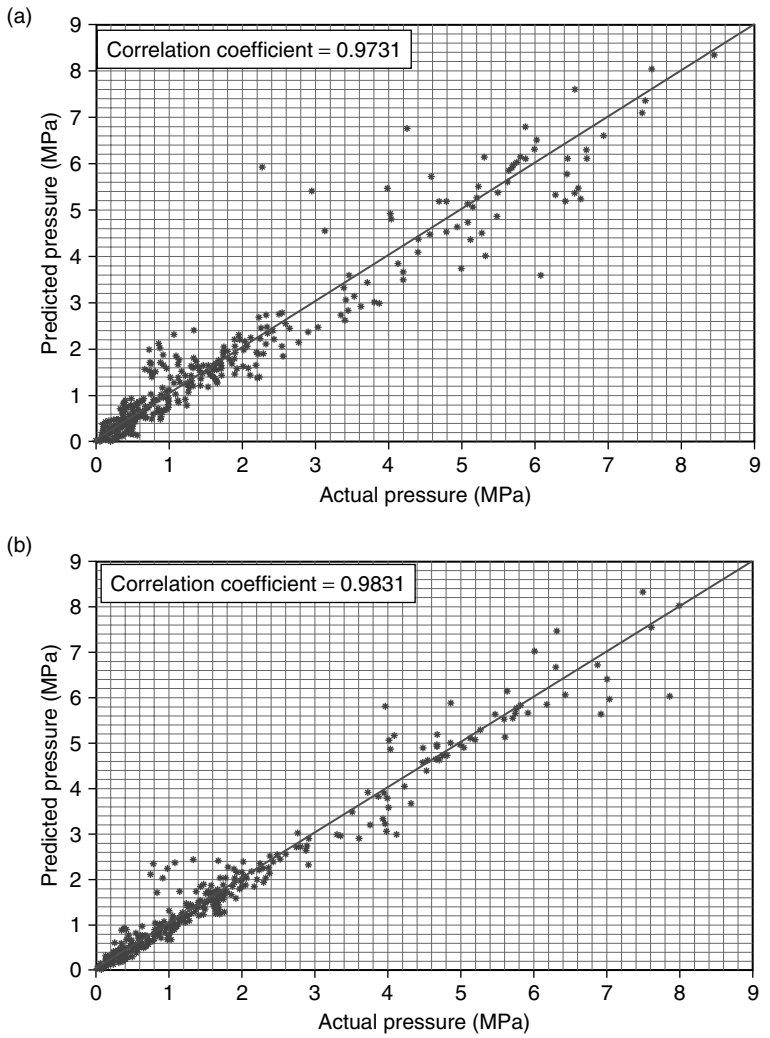

Figure 5. Peak pressure results for (a) scaled input (5 input variables) and (b) non-scaled input (6 input variables)

The non-scaled version produces better results than the scaled version. This is not an implication on the validity of the practice of cubed-root scaling, but rather a depiction of the ability of the ANN to learn the training patterns. When cube-root scaling is applied, the errors due to the charge size are hidden in the other variables. With the 6 variables, the ANN is able to learn the patterns better. Therefore, all following work was performed without the use of cube-root scaling.

4.3. APPROACH TWO: BIASED SPACING OF TRAINING GRID

Analysis of the results from approach one showed a bias of the absolute errors towards the base of the structure, in particular for points below the height of the barrier, as depicted in

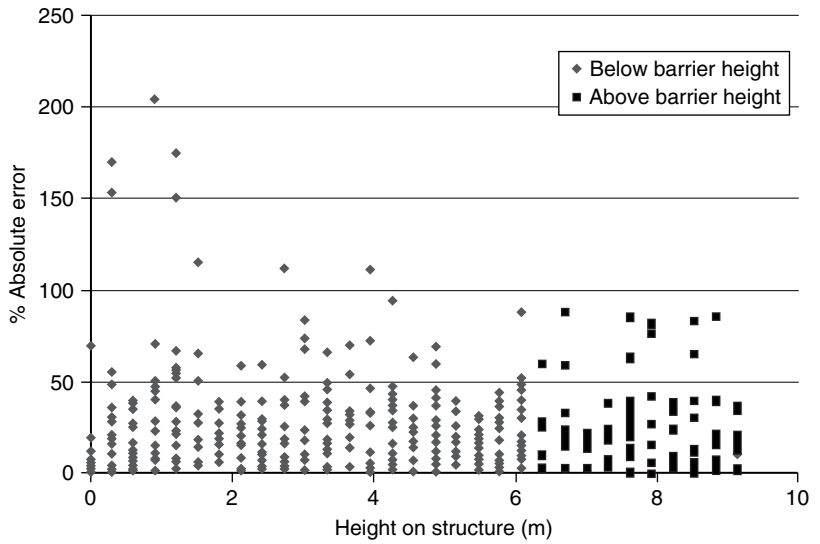

Figure 6. Bias of peak pressure errors towards heights on the structure face below the height of the blast wall

respect to peak pressure predictions in Figure 6. To address this problem, the second approach used tracer points that were biased in location on the face of the structure towards its base. The location of the tracers on the width of the structure remained the same, however. This provided the ANN with more training data in the areas that had shown the greatest absolute errors in the peak pressure predictions.

Table 2 shows the comparison of the behavior of the evenly spaced grid in comparison with the biased grid with 500 hidden neurons.

Table 2. Statistical comparison of an evenly distributed grid of training points and a biased grid

ANN	Correlation factor		MAE		RMSE		Std deviation		Kurtosis	
model	**Even**	**Bias**	**Even**	**Bias**	**Even**	**Bias**	**Even**	**Bias**	**Even**	**Bias**
Pressure (MPa)	0.981	0.987*	0.06	0.04*	0.21	0.17*	1.09	1.06*	15.07	14.8*
Impulse (MPa-ms)	0.993	0.995*	0.04*	0.08	0.42	0.36	3.79	3.78	4.13	3.74*
Time of Arrival (ms)	0.980*	0.979	0.86*	1.41	5.25*	5.36	26.9	26.7*	3.76	3.40*
Duration (ms)	0.968*	0.961	2.22	1.92*	7.96	8.78	31.6*	31.8	–0.31	–0.24*

Statistical Measure NB: *indicates winning pattern set.

The analysis of biasing the grid of training points lower on the structure face produces some interesting results. The peak pressure ANN is improved by all accounts when using the biased grid. The correlation is stronger, the mean absolute error (MAE) is reduced and it shows a more linear behavior with fewer large error occurrences. The impulse ANN is also improved by biasing the grid with the exception of the MAE which doubles. Despite the MAE increase, it shows a more linear distribution with fewer occurrences of large errors. There are more occurrences of small errors, but the general fit is better. The time of arrival ANN has stronger correlation, and smaller MAE and root mean square error (RMSE) for the evenly spaced grid, although the standard deviation and kurtosis are better with the biased grid. The evenly spaced grid shows better correlation in general, but the biased grid shows better results for high values of the time of arrival. The duration ANN shows better results for the evenly spaced grid despite a lower MAE with the biased grid.

4.4. APPROACH THREE: EFFECT OF ADDITIONAL TRAINING PATTERNS

The aim of the third approach is to explore the value in expanding the amount of data within the variable space used to train the ANN models. As described in Section 4.1, increasing the density of training patterns should increase the accuracy of the ANN model. In addition to the primary 81 simulations that were generated, 5 additional simulations were completed, with randomly selected values for W, d_1, Z, and H, to use for the study of the effect of the number of training patterns. In particular, these experiments would indicate whether increasing from a $3 \times 3 \times 3 \times 3$ grid to a $5 \times 5 \times 5 \times 5$ grid (that is, increasing the number of simulations performed to generate training patterns from 81 to 625) would be worth the time and computational cost.

Table 3 indicates that the ANN models are improved in almost every aspect with the addition of the five extra simulations from which several additional training patterns were selected. The standard deviation and kurtosis are slightly higher for the impulse ANN, but all other measures are less. Figure 7 indicates that the impulse ANN is learning better with the extra training patterns. All measures suggest that expanding to a $5 \times 5 \times 5 \times 5$ grid, if possible, will yield significantly improved results.

Table 3. Statistical comparison of biased grid models and the biased grid models with 5 extra simulations

ANN	Correlation factor		MAE		RMSE		Std deviation		Kurtosis	
model	**Extra**	**Bias**	**Extra**	**Bias**	**Extra**	**Bias**	**Extra**	**Bias**	**Extra**	**Bias**
Pressure (MPa)	0.990*	0.987	0.012*	0.040	0.154*	0.173	1.065	1.061*	14.74*	14.78
Impulse (MPa-ms)	0.996*	0.995	0.053*	0.080	0.339*	0.355	3.782	3.775*	3.87	3.74*
Time of Arrival (ms)	0.977	0.979*	1.269*	1.414	5.666	5.356*	26.82	26.72*	3.77	3.40*
Duration (ms)	0.963*	0.961	0.337*	1.918	8.549*	8.781	31.73*	31.81	–0.23*	–0.24

Statistical Measure NB: *indicates winning pattern set.

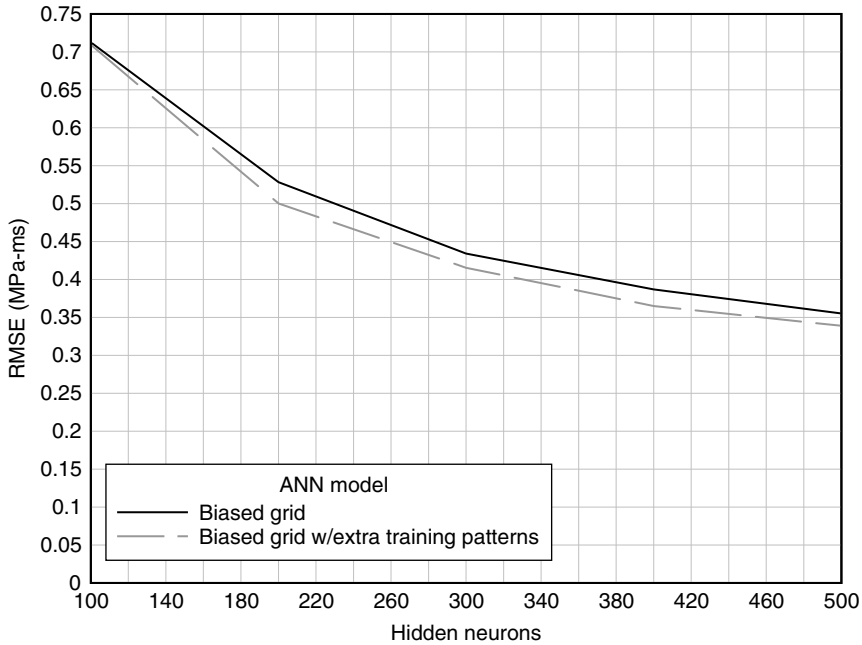

Figure 7. Training progression of impulse ANN compared to the model with extra training patterns

4.5. TESTING

The approaches presented to this point have been compared using data that exists at points between the tracers used for training the ANN models. It is also important, however, to gauge the behavior of the ANN models against a blind set of data that exists in the variable space between the blast wall and structure configurations used to train the ANN models. To this end, 5 additional randomly generated test simulations were completed to gauge the effectiveness of the ANN models to the test data. The configurations of the test simulations are outlined in Table 4 and can be compared against the variable extents in Table 1.

The test produces mixed results. The peak pressure is the most accurate followed by the time of arrival, impulse, and the positive phase duration respectively. Table 5 displays the behavior and Figure 8 and Figure 9 show the performance of the peak pressure and the impulse ANN models.

Table 4. Test simulation configurations

W (kg-TNT)	h (m)	d1 (m)	Z (m)
680.87	2.64	7.14	29.17
586.62	2.35	5.16	22.31
839.80	3.98	5.16	14.30
560.65	4.60	0.93	7.36
128.99	4.14	7.38	20.67

Table 5. Comparison of ANN model correlation with test data

ANN model	Correlation factor	MAE	RMSE	Standard deviation	Kurtosis
Peak Pressure (MPa)	0.942	0.044	0.117	0.343	1.229
Impulse (MPa-ms)	0.784	1.486	1.743	2.495	–0.999
Time of Arrival (ms)	0.851	2.010	5.820	15.555	–1.430
Duration (ms)	0.504	24.984	27.067	17.534	–0.633

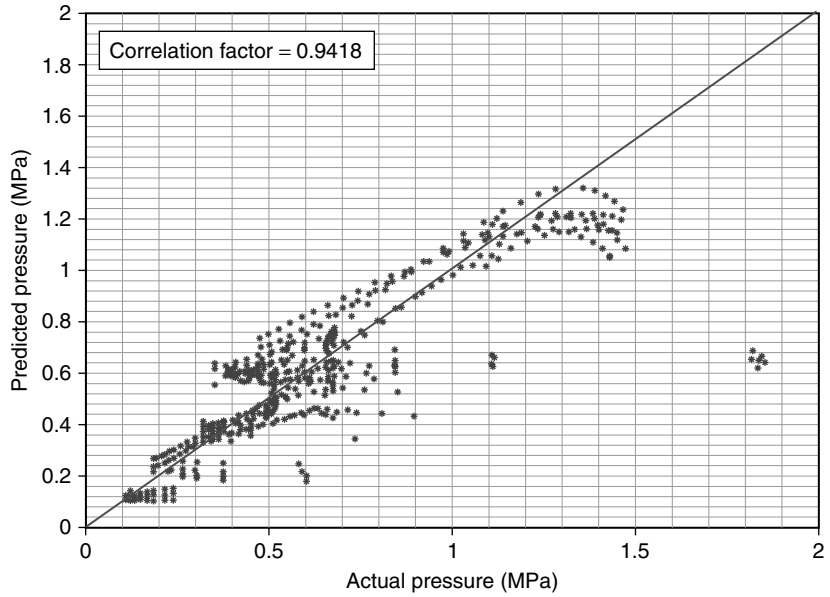

Figure 8. Correlation of ANN model with test data for peak pressure

The results tend to be in line with what might be expected. The peak pressure and the time of arrival are the most accurate, which is intuitive because these values are not as likely to be effected by multiple reflections. The impulse and duration however are very susceptible to errors due to multiple reflections and their performance is less accurate than the ANN models for pressure and time of arrival.

4.6. PREDICTION OF ROOF LOADS

Blast loads applied to roof structures are predicted by applying an increase factor to the free-field incident pressure based on the standoff, height of the building, and the length of the building to be loaded as shown in Figure 10 [10].

In contrast to vertical wall reflected pressures where the air pressure has a sudden jump from atmospheric pressure up to the peak reflected pressure, roof load predictions are defined as a rise to the peak pressure over time followed by an unequal decay of the blast pressures [10]. In a free-field situation, roof loads are predictable. In a situation with a protective blast wall in front of a structure, the predictability of the roof loads is dependent upon the configuration of W, d_1, Z, and h_s.

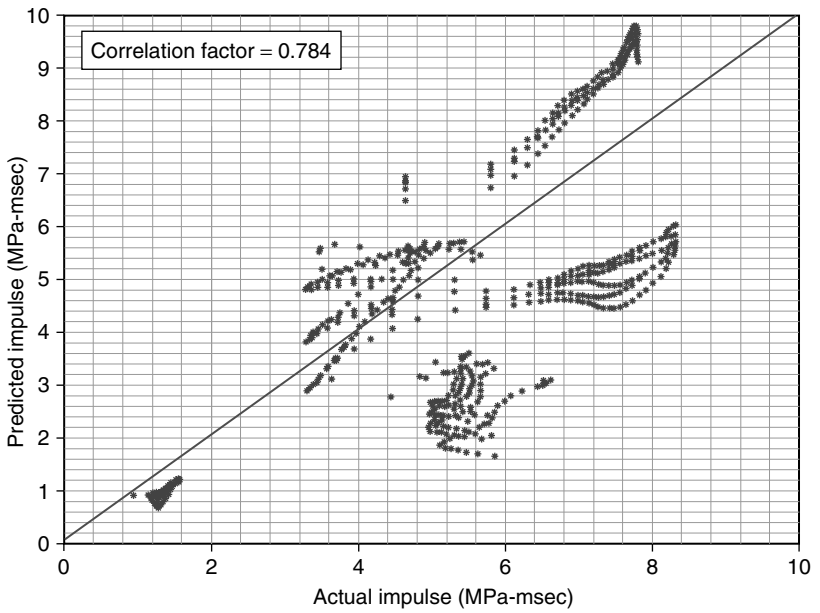

Figure 9. Correlation of ANN model with test data for impulse

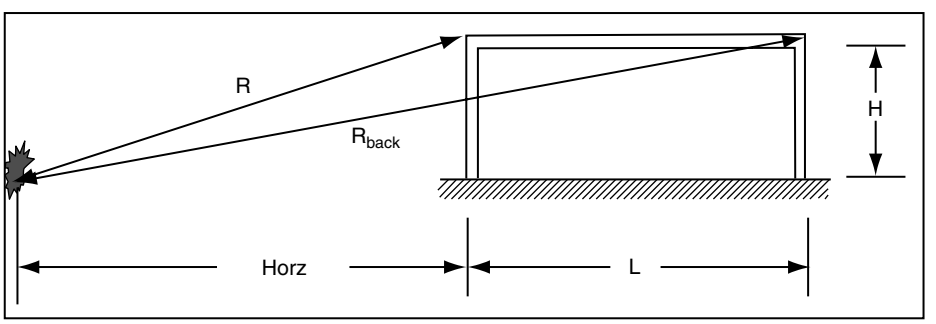

Figure 10. Factors for predicting blast loading to roofs

In order to study the effects of protective blast walls on the blast loading of roofs, data on the first 1.524 *m* of the structures were collected during all of the simulations generated for the structure loading ANN's formulated in this work. A pragmatic evaluation of the variables provides insight into the effects on the properties that define a blast loading. In general, the peak pressure and time of arrival are less affected by the presence of a blast wall as opposed to the impulse and duration. This is seen in the results from the roof load ANN development (Table 6).

The ANN models for peak pressure, time of arrival, and duration all show good correlation and display improvement with the addition of extra training patterns as outlined in previous sections. The impulse ANN does not show good correlation. Other than the standard deviation being decreased, all the statistical measures become worse by the addition of extra training patterns for the impulse ANN model.

Table 6. Comparison of ANN model predictions with test data

ANN model	Correlation factor		MAE		RMSE		Std deviation		Kurtosis	
	Even	**Extra**	**Even**	**Extra**	**Even**	**Extra**	**Even**	**Extra**	**Even**	**Extra**
Pressure (MPa)	0.989*	0.989	0.038	0.034*	0.014	0.014	0.071	0.071	9.20	9.06*
Impulse (MPa-ms)	0.627*	0.601	0.009*	0.031	1.191*	1.214	1.099	1.094*	156.8*	159.8
Time of Arrival (ms)	0.942	0.948*	9.629	0.501*	3.758	3.548*	21.1*	21.2	3.693	3.617*
Duration (ms)	0.886	0.903*	3.18*	9.46	7.28	6.76	34.1	33.2*	–0.46	–0.42*

Statistical Measure NB: *indicates winning pattern set.

5. DISCUSSION

In all the cases as discussed above, the pressure and time of arrival functions are captured by the ANN approach. The impulse and positive phase duration ANNs are less accurate however. The results suggest that it would be beneficial to increase the number of training patterns input into the neural networks. The current results are produced using a $3 \times 3 \times 3 \times 3$ grid covering the variable data space. The $3 \times 3 \times 3 \times 3$ grid represents 81 experiments with 30 data points embedded in each experiment for a total of 2,430 training patterns. Increasing to a $5 \times 5 \times 5 \times 5$ grid of the variable data space would increase the number of experiments to 625 with 30 data points embedded in each experiment for a total of 18,750 training patterns.

The implications of increasing the density of the grid of training data is the difficulty in generating the amount of data required. The problem is magnified when the bounds of the model are desired to be expanded from the current range. By examining the charge weight variable, the implications can be demonstrated. The current range for the charge weight is 22.68 kg to 910.42 kg. Assuming an evenly distributed grid spacing, the density for a 3×3 grid would require experiments with the charge weight incremented 443.87 kg. Increasing to the $5 \times 5 \times 5 \times 5$ grid would have the charge weight incremented by 221.935 kg. After the $5 \times 5 \times 5 \times 5$ grid is established, the bounds of the model can be extended by maintaining a consistent density of the data in the grid of training data. Thus, for each 221.35 kg incremental increase in the range of the charge weight, there will be 256 (4^4) experiments required to maintain a consistent density.

The computational modeling used to produce the simulations for the $3 \times 3 \times 3 \times 3$ grid was completed using DoD supercomputers. The simulations ranged from 12 processors up to 164 processors with an average wall clock time of 60 hours. The total number of processor hours, equal to the number of processors multiplied by the wall clock time, required for the simulations populating the $3 \times 3 \times 3 \times 3$ grid of data was approximately 1.5 million hours. This exhibits both the large investment required to produce accurate numerical simulations and the need for a quick engineering tool for efficient and accurate predictions. The limitations of applying a neural network modeling technique reside predominantly in the investment to produce the data required for training the ANN model.

The approach developed in this work were compared against simulation runs that were held back during the training process and used for testing. The ANN approach provides

pertinent design information for blast pressure loading to structures behind blast barrier walls that could be useful for design of the structures. The approach has not been validated against existing live blast test data. This is a step that would be needed to be addressed before the method could be validated as a design tool.

6. CONCLUSION

Blast design and assessment of structures protected by blast barrier walls require aids to develop beneficial configurations. CFD modeling, as demonstrated, can be a very accurate approach to predict blast wave and structure interaction. In order to produce those accurate results, there is a very large overhead of hardware requirements, modeling expertise, and wall clock time. ANNs provide an efficient tool to aid in optimizing site layout and structural design for terrorist type threats. The advantage of the ANN approach is that it can provide good results in a fraction of a second, allowing optimal design solutions to be sought. The downside is that ANNs require a large set of data to achieve acceptable levels of accuracy, and this data set can be expensive to collect.

The results of this study show the development of an ANN methodology for a range of values for the variables of charge weight, charge to barrier standoff, barrier to structure standoff, barrier height, and location on the structure face as well as roof loads. The development was performed on a $3 \times 3 \times 3 \times 3$ grid of the variable data space. Experience and the results of this study show that moving to a $5 \times 5 \times 5 \times 5$ grid of the variable space would provide improved results. The significance of this study is that it displays the ANN technology at the edge of its applicability. A total of 81 simulations were required for the $3 \times 3 \times 3 \times 3$ grid, whereas 625 would be required for a $5 \times 5 \times 5 \times 5$ grid. The $5 \times 5 \times 5 \times 5$ grid would provide improved results for the bounds of the current problem. Furthermore, if the scope of the model was to be expanded in terms of the range of the variables, then a corresponding increase in the size of the training data set would be required if the same level of accuracy was to be maintained

The ANN technology shows the capability to model the nonlinear blast loading function in an environment with a blast barrier protective wall. The ANN performance has been presented for a $3 \times 3 \times 3 \times 3$ grid of the variable space. There are differing degrees of non-linearity for the predicted values of each of the variables considered. Peak pressure and time of arrival show the most predictable responses. Impulse and positive phase duration have a higher degree of non-linearity that proves more difficult for the ANN approach to learn. Based on the 6 input variables (W, d_1, Z, H, w_s, and hs) the ANN provides a fast-running tool that is able to give an idealized blast load to structural components.

REFERENCES

1. W.E. Baker. *Explosions in Air*. University of Texas Press (Austin) 1973.
2. T.A. Rose, P.D. Smith, and G.C. Mays. The Effectiveness of Walls Designed for the Protection of Structures Against Airblast From High Explosives, *Proceedings of the Institution of Civil Engineers – Structures and Buildings,* 1995; 110:78–85.
3. T.A. Rose, P.D. Smith, and G.C. Mays. Design Charts Relating to Protection of Structures Against Airblast From High Explosives, *Proceedings of the Institution of Civil Engineers – Structures and Buildings*, 1997; 123:186–192.
4. *UFC 4-020-03, Security Engineering Final Design*. Departments of the Army and the Air Force, May 1994.
5. D. Bogosian and S. Yongjiang. An Enhanced Methodology for Predicting Loads behind Blast Barriers, *74th Shock & Vibration Symposium*, October 2003, San Diego, California.
6. D. Bogosian and S. Yongjiang. *Assessment of and Predictive Methodology for Blast Barrier Effectiveness, TR-01-34,* Karagozian & Case, January 2002.

7. D. Rickman and D. Murrell. *Miniature-Scale Experiments of Airblast Diffraction Over Barrier Walls: Results and Analysis, ERDC/GSL TR 04-2*, USACE Engineering Research and Development Center, Vicksburg, MS.
8. D. Rickman, D. Murrell, and B. Armstrong. Improved Predictive Methods for Airlbast Shielding by Barrier Walls, *ASCE Structures Congress*, May 2006, St. Louis, MO.
9. X.Q. Zhou and H. Hao. Prediction of Airblast Loads on Structures Behind a Protective Barrier. *Int J of Impact Eng* 2008; 35:363–375.
10. *TM5-1300, Structures to Resist the Effects of Accidental Explosions*. US Department of the Army; 1990.
11. *UFC 3-340-01, Design and Analysis of Hardened Structures to Conventional Weapons Effects*. US Army Corps of Engineers, Naval Facilities Engineering Command, Air Force Civil Engineering Support Agency; 1 June 2002.
12. J.O. Hallquist. *LS-DYNA3D Theoretical Manual*. Livermore Software Technology Corp. LSTC Report 1018 Rev. 2, Livermore Software Tech, Livermore, CA, rev July 1993.
13. Century Dynamics. *AUTODYN 2-D & 3-D User's Manual*, 2003.
14. R. Löhner, C. Yang, J.D. Baum, and E. Mestreau. Advances in FEFLO. *AIAA-02-1024*, American Institute of Aeronautics & Astronautics, 2002.
15. T.A. Rose. *Air3D user's guide. 7.0*: RMCS. UK: Cranfield Unversity; 2003.
16. J. Crepeau, C. Needham, and S. Hikida. *SHAMRC Second-Order Hydrodynamic Automatic Mesh Refinement Code. Methodology, Vol. 1*. Albuquerque, NM: Applied Research Associates, Inc.; 2001.
17. J. Crepeau. *SHAMRC Second-Order Hydrodynamic Automatic Mesh Refinement Code. User's Manual, Vol. 2*. Albuquerque, NM: Applied Research Associates, Inc.; 1998.
18. J.M. McGlaun, S.L. Thompson, and M.G. Elrick. CTH: A Three-Dimensional Shock Physics Code. *Int J Impact Eng* 1990; 10:351–60.
19. R. McKeown, O. Dengel, G. Harris, and H.J. Diekhoff. *Development and Evaluation of DYSMAS Hydrocode for Predicting Underwater Explosion Effects. Executive sSummary, Vol. I, IHTR 2492*. Naval Surface Warfare Center (NSWC), Indian Head, MD, February 2004.
20. I. Flood, B. Bewick, R. Dinan, and H. Salim. Modeling Blast Wave Propagation Using Artificial Neural Network Methods. *Advanced Eng Informatics* 2009; 23:418–423.
21. R. Löhner, J.D. Baum, and D. Rice. Comparison of Coarse and Fine Mesh 3-D Euler Predictions for Blast Loads on Generic Building Configurations. In: *Proc MABS-18*, Bad Reichenhall, Germany, September 2004.
22. I. Flood and N. Kartam. Neural Networks in Civil Engineering. I: Principals and Understanding. *J of Computing in Civil Engineering*, 1994; 8(8):131–148.
23. I. Flood and N. Kartam. Neural Networks in Civil Engineering. II: Systems and Application. *J of Computing in Civil Engineering*, 1994; 8(8):149–162.
24. A.M. Remennikov and T.A. Rose. Predicting the Effectiveness of Blast Barrier Walls Using Neural Networks, *Int J of Impact Engineering*, 2007; 34:1907–1923.
25. C.E. Needham. Blast Loads and Propagation Around and Over a Building. *26th International Symposium on Shock Waves*, Gottingen, Germany, July, 2007.
26. C.W. Mastin, B.J. Armstrong, and C.W. Welch. Verification of the CTH Hydrocode Against the Kingery and Bulmash Data Sets. In: *Lim Proc 66th S&V*, October 1995. p. 121–9.
27. Naval Surface Warfare Center (NSWC). *GEMINI: The DYSMAS Euler Solver User's Manual* (release 4.46), Indian Head, MD, April 2008.
28. M. Roth, J. Bennet, W. Heard, and R. Stinson. CFD Modeling of Blast Intrusion into Field Fortifications. In: *Proc 77th S&V*, October 2006.
29. P.J. Roache. *Verification and Validation in Computational Science and Engineering*. Hermosa Publishers; 1998.
30. P.J. Roache. Perspective: A Method for Uniform Reporting of Grid Refinement Studies. *ASME J of Fluids Eng*, 1994; 116:405–413.
31. L. Schwer, M. Saadeghvaziri, J. O'Daniel, and T. Madsen. Free-Air Blast Simulation: Engineering Model and MM-ALE Calculations. In: *Proc MABS 20*, Oslo, Norway 2008.
32. I. Flood. Modeling Dynamic Engineering Processes Using Radial-Gaussian Neural Networks. *J of Intelligent and Fuzzy Systems,* 1999; 7:373–385.